

KCNQ2/3/5 channels in dorsal root ganglion neurons can be therapeutic targets of neuropathic pain in diabetic rats

Ting Yu^{1, 2}, Lei Li³, Huaxiang Liu⁴, Hao Li⁵, Zhen Liu¹, Zhenzhong Li¹

¹Department of Anatomy, Shandong University School of Basic Medical Sciences, Jinan, China

²Department of Physiology, Jining Medical University, Jining, China

³Department of Diagnosis, Jining Medical University, Jining, China

⁴Department of Rheumatology, Shandong University Qilu Hospital, Jinan, China

⁵Department of Orthopaedics, Shandong University Qilu Hospital, Jinan, China

Corresponding author:

Zhenzhong Li, Department of Anatomy, Shandong University School of Basic Medical Sciences,
44 Wenhua Xi Road, Jinan, Shandong Province 250012, China.

Email: zli@sdu.edu.cn

Abstract

Background: Diabetic neuropathic pain is poorly controlled by analgesics and the precise molecular mechanisms underlying hyperalgesia remain unclear. The KCNQ2/3/5 channels expressed in dorsal root ganglion (DRG) neurons are important in pain transmission. The expression and activity of KCNQ2/3/5 channels in DRG neurons in rats with diabetic neuropathic pain were investigated in this study.

Methods: The mRNA levels of KCNQ2/3/5 channels were analyzed by real-time polymerase chain reaction (PCR). The protein levels of KCNQ2/3/5 channels were evaluated by Western blot assay. KCNQ2/3/5 channel expression in situ in DRG neurons was detected by double fluorescent labeling technique. M current (I_M) density and neuronal excitability were determined by whole-cell voltage and current clamp recordings. Mechanical allodynia and thermal hyperalgesia were assessed by von Frey filaments and plantar analgesia tester, respectively.

Results: The mRNA and protein levels of KCNQ2/3/5 channels significantly decreased, followed by the reduction of I_M density and elevation of neuronal excitability of DRG neurons from diabetic rats. Activation of KCNQ channels with retigabine (RTG) reduced the hyperexcitability and inhibition of KCNQ channels with XE991 enhanced the hyperexcitability. Administration of RTG alleviated both mechanical allodynia and thermal hyperalgesia, while XE991 augmented both mechanical allodynia and thermal hyperalgesia in diabetic neuropathic pain in rats.

Conclusion: The findings elucidate the mechanisms by which downregulation of the expression and reduction of the activity of KCNQ2/3/5 channels in diabetic rat DRG neurons contribute to neuronal hyperexcitability, which results in hyperalgesia. These data provide intriguing evidence that activation of KCNQ2/3/5 channels might be the potential new targets for alleviating diabetic neuropathic pain symptoms.

Keywords

KCNQ channels; retigabine; XE991; neuron; dorsal root ganglion; diabetic neuropathy

Introduction

KCNQ channels are voltage-dependent potassium channels composed of different combinations of four subunits that differently expressed in the peripheral and central nervous system [1-5]. It is known that KCNQ channels have potential therapeutic value by targeting their activity [6, 7]. The differentially expressed KCNQ subunits have a direct role in regulating excitability of the neurons that they are distributed [2]. It has been anticipated that by targeting KCNQ channels for development of new drugs on neuronal excitability will be a breakthrough on improving neuronal diseases [8]. KCNQ channels are widely expressed in nociceptive dorsal root ganglion (DRG) neurons and are important for controlling neuronal excitability. Activation of KCNQ channels has proven to be effective on reducing pain in peripheral nerve injury and inflammation models [9, 10].

Due to their particular characteristics, KCNQ channels have been shown to have pronounced control over the excitability of neurons. The dynamic surface expression of the KCNQ channels is highly modulated by neurotransmitters and neural activity. The altered KCNQ activity contributes to different neuronal hyperexcitability related pathological conditions [11]. KCNQ channels form a slow non-inactivating K^+ current, also known as the M current (I_M). They activate in the subthreshold range of membrane potentials and regulate different aspects of excitability in neurons [12, 13]. The KCNQ mediated I_M regulates excitability of peripheral sensory nociceptors in the pain pathways [3, 14]. I_M is known to be provoked on key areas on neuronal surface to control action potential (AP) initiation and propagation [11]. Therefore, how the I_M is affected during diabetic neuropathy and whether it is involved in the effect of KCNQ channels is still unknown. Chronic pain after injury is highly resistant to available treatments [10]. Diabetes is the most common cause of neuropathy [15,16]. Diabetic neuropathy is the most usual complication of diabetes [17-20]. Diabetic neuropathic pain is one of the main symptoms, however, currently available drugs are often ineffective and complicated by adverse events [18, 21-24]. Neuropathic pain is a frequently encountered condition that is often resistant to treatment and is associated with poor patient satisfaction of their treatment. The management of chronic neuropathic pain is challenging [25] and is best achieved with the use of effective targets related to the main mechanisms associated with pain transduction. The spinal cord and even much higher level of the central nervous system are also involved in generation of diabetic neuropathic pain [26-29]. The

key pathological alteration of diabetic neuropathy is the gradually damaged peripheral nerve terminals [30]. Hence, by targeting the central nervous system as the diabetic neuropathic pain administration may have some limitations involved. By focusing on the peripheral nervous system, the neuromodulation modality of DRG stimulation is suggested as diabetic neuropathic pain improving indication [31]. The possibility that activators of KCNQ channels could be useful for treating chronic pain is strongly supported by electrophysiological evidence and pharmacological experiments [10]. As the KCNQ channel opener, retigabine (RTG) induced I_M in different types of neurons and inhibited pathological hyperexcitability AP firing in several different experimental conditions [2, 3, 32-35]. RTG have been suggested to treat nociception modulated by I_M and relieved neuropathic pain provoked by stimulation of afferent neurons [3, 34]. XE991 blocked the KCNQ induced I_M and therefore potentiated the hyperexcitability in several different experimental conditions [3, 20, 32, 33, 36, 37]. Therefore, we investigated the effects of RTG administration on neuronal excitability in DRG afferent neuronal activities of diabetic neuropathic rats as well as the effects of RTG treatment on pain nociceptive behavior of diabetic neuropathic rats. In addition, the effects of XE991 on neuronal excitability and neuropathic behavior of diabetic neuropathic rats were also evaluated in order to fully investigate the involvement of KCNQ2/3/5 channels in nociceptive sensory transduction of diabetic neuropathic pain. These data provide evidence that KCNQ2/3/5 channels might be the potential new targets for relieving diabetic neuropathic pain, a medical condition for which few effective therapeutic options are available.

Materials and methods

Diabetic neuropathic pain animal model

All the animals involved in the present study were male Wistar rats (from the Experimental Animal Center at Shandong University of China) weighing 200-250 g. All animals were cared for in accordance with the National Institute of Health Guide for the Care and Use of Laboratory Animals (eighth edition, 2010; International Standard Book Number-13: 978-0-309-15400-0; <http://www.nap.edu>). All procedures described herein were reviewed by and had prior approval by the Ethical Committee for Animal Experimentation of the Shandong University. Animals were housed in plastic cages in groups of 4 at room temperature on a 12-h light/dark cycle with free access to food and water. All surgery was performed under anesthesia, and all efforts were made to

minimize animal suffering, to decrease the number of animal used, and to utilize alternatives to in vivo experiments of the animals. The diabetic rats were induced by a single intraperitoneal injection (i.p.) of streptozotocin (STZ; Sigma, St. Louis, MO, USA; 55 mg/kg freshly dissolved in 0.1 mol/L citric acid buffer, pH 4.5). Age-matched rats injected with the same volume of the vehicle were used as controls. The diabetic neuropathic pain rats were defined as a blood glucose level ≥ 20 mmol/L from 3 days to 8 weeks after STZ treatment and with evident neuropathic pain (mechanical threshold ≤ 5.0 g and withdrawal latency ≤ 10 s) at 8 weeks after STZ administration. All the animal groups and following experimental design were randomized.

Tissue collection for analysis

After 8 weeks of STZ or vehicle injection, the baseline pain behaviors were tested. After that, the animals were anesthetized with 3% sodium pentobarbital (1 ml/kg body weight, i.p.). Bilateral L4-6 dorsal root ganglia (DRGs) were removed from each animal. These DRGs were processed for real-time quantitative polymerase chain reaction (PCR), Western blot assay, and double fluorescent staining to analyze the expression of KCNQ2/3/5 channels in both mRNA and protein levels, and were isolated to single cell to perform patch clamp recording to examine I_M .

Real-time PCR analysis of KCNQ2/3/5 channel mRNA expression in DRG

After DRGs were removed from each animal, the mRNA levels of KCNQ2/3/5 channels in L4-6 DRGs were analyzed by real-time PCR with β -actin mRNA as an internal control. Total RNA from tissues was extracted by TRIzol (Takara, Japan). Reverse transcription was performed using cDNA synthesis kit (Thermo Scientific Molecular Biology, Lithuania, EU). The primers (Sangon Biotech, Shanghai, China) are targeted to different parts of the sequence of KCNQ: KCNQ2 (718-902), KCNQ3 (1303-1444), and KCNQ5 (1163-1408). When we tested these primers with conventional PCR, only one band at the appropriate target size was detected. The primer sequences for KCNQ2/3/5 channels and β -actin were: KCNQ2 5'- GCT TGC GGT TCT TAC AAA TCT T -3' (forward) and 5'- GTG GTC ATT CTC ACC CTT TTC T -3' (reverse). KCNQ3 5'- CCA AGG AGA GGA AAT GAA AGA G -3' (forward) and 5'- TAAAGA AAA GGT GGC AGC AAT C -3' (reverse). KCNQ5 5'- CTT CGC CCT TCT TGG TAT TTC T -3' (forward) and 5'- TCC CCT TGT TCT TTC TTG GTAG -3' (reverse). β -actin 5'-CAC CCG CGA GTA CAA

CCT TC -3' (forward) and 5'- CCC ATA CCC ACC ATC ACA CC-3' (reverse). The amplification was conducted in a volume of 25 μ l containing 12.5 μ l of Maxima SYBR Green qPCR Maxter Mix (2 \times) (Thermo Scientific Molecular Biology, Lithuania, EU), with 0.3 μ mol/L forward and reverse primers, 2 μ l cDNA. Real-time RT-PCR was performed using the Eppendorf Realplex PCR system (Eppendorf, Hamburg, Germany). The PCR cycle conditions were as follows: activation at 95°C for 10 minutes, amplification and quantification for 40 cycles at 95°C for 15 seconds, 60°C for 30 seconds, and 72°C for 30 seconds. The comparative cycle of threshold fluorescence (Ct) method was used to obtain the relative transcript amount of the target gene by normalizing it to that of β -actin with Δ Ct values.

Western blot assay of KCNQ2/3/5 channel protein expression in DRG

Upon DRG removal, the protein levels of KCNQ2/3/5 channels in L4-6 DRGs were determined by Western blot assay. The DRGs were homogenized with Radio Immunoprecipitation Assay (RIPA) Buffer (Beyotime, Haimen, China) and the protein concentration was determined using a BCA Protein Assay Kit (Beyotime, Haimen, China). Samples containing 50 μ g protein were loaded onto the 10% SDS gel, separated by electrophoresis and transferred to nitrocellulose (NC) membrane. The membranes were blocked in 5% bovine serum albumin (BSA) and then were incubated with mouse anti-KCNQ2 monoclonal IgG (1:1,000, Abcam, Cambridge, MA), rabbit anti-KCNQ3 polyclonal IgG (1:1,000, Chemicon, Temecula, CA), rabbit anti-KCNQ5 polyclonal IgG (1:1,000, Chemicon, Temecula, CA), and mouse anti- β -actin monoclonal IgG (1:1,000, Santa Cruz Biotechnology, Santa Cruz, CA), respectively, overnight at 4°C. The membranes were washed for 3 times and incubated with goat anti-rabbit IgG-HRP (1:4,000, Santa Cruz Biotechnology, Santa Cruz, CA) or goat anti-mouse IgG-HRP (1:4,000, Santa Cruz Biotechnology, Santa Cruz, CA). The immunoreactive bands were visualized with an enhanced chemiluminescent detection kit (Millipore Corporation, Billerica, MA) in the FluorChem E Digital Darkroom (Bucher Biotec, Switzerland). The images were analyzed by the AlphaView software (Version: 3.4.0.0). The protein levels of KCNQ2/3/5 were expressed as the ratio of the protein to β -actin.

Double fluorescent labeling of KCNQ2/3/5 channels in DRG sections

The L4-5 DRGs were removed from each animal and fixed with 4% paraformaldehyde for 4 hours

at 4°C. After that, the DRG explants were sectioned by a freezing microtome (AS620 Cryotome, UK) at the thickness of 20 µm. DRG sections were processed for double fluorescent labeling of KCNQ2/3/5 channels with a neuron marker microtubule-associated protein 2 (MAP2) or KCNQ2/3/5 channels with a nociceptive neuron marker transient receptor potential vanilloid type-1 (TRPV1). A blocking and permeabilizing solution, which contained 10% normal goat serum in 0.3% Triton phosphate buffer saline (PBS), was used to block non-specific sites and permeabilize cells. The sections were incubated with mouse monoclonal anti-KCNQ2 (1:400, Abcam, Cambridge, MA), rabbit polyclonal anti-KCNQ3 (1:300, Chemicon, Temecula, CA), rabbit polyclonal anti-KCNQ5 (1:300, Chemicon, Temecula, CA), chicken polyclonal anti-MAP2 (1:2000, Abcam, Cambridge, MA), and sheep polyclonal to TRPV1 (1:500, Abcam, Cambridge, MA, USA), respectively, overnight at 4°C. After washing in 0.1 mol/L PBS for 3 times, the sections were incubated with goat anti-rabbit conjugated to Cy3 (1:200, Abcam, Cambridge, MA), goat anti-mouse conjugated to Cy3 (1:200, Abcam, Cambridge, MA), goat anti-chicken conjugated to Cy2 (1:200, Abcam, Cambridge, MA), rabbit anti-mouse conjugated to Cy3 (1:200, Invitrogen Corporation, Grand Island, NY), rabbit anti-sheep conjugated to Cy2 (1:200, Jackson ImmunoResearch, West Grove, PA), mouse anti-rabbit conjugated to Cy3 (1:200, Invitrogen Corporation, Grand Island, NY), and mouse anti-sheep conjugated to Cy2 (1:200, Jackson ImmunoResearch, West Grove, PA) for 60 minutes in darkness, respectively. The sections were rinsed in 0.1 mol/L PBS and covered with Vectashield anti-fade mounting medium (Vector Laboratories, Burlingame, CA). All images were captured by Olympus fluorescent microscope. The Image Pro Plus (version 6.0, Media Cybernetics, Silver Spring, MD) image analyzing software was used to analyze the DRG sections. The proportion of KCNQ2/3/5 channel positive neurons and their relative fluorescence intensity were calculated in a blind fashion. Three consecutive sections (100-µm interval) of each DRG from 5 animals in each group were analyzed. Six adjacent fields from the same section were considered to be one observation. The relative fluorescence intensity was the mean optical density within each DRG section.

Cell culture and patch-clamp recording

The DRG explants were digested with 0.5% trypsin (Sigma, St. Louis, MO) and 1% collagenase (type IA, Invitrogen Corporation, Grand Island, NY) in D-Hanks solution at 37°C for 1 hour and

isolated to single cell. After dissociation, 10% fetal bovine serum (Invitrogen Corporation, Grand Island, NY) was added to stop digestion, and the cells were centrifuged for 10 minutes at 1,000 rpm. The dissociated cells were resuspended in DMEM/F-12 (Gibco, Grand Island, NY), which consisted of 10% fetal bovine serum and placed on 24-well sterile clusters containing poly-L-lysine (0.1 mg/ml, Sigma, St. Louis, MO) precoated glass coverslips and kept in 5% CO₂ incubator at 37°C before use. Recordings were performed within 24 hours after plating. Whole-cell voltage and current clamp recordings were performed at room temperature (20°C~22°C) using an EPC-9 amplifier and Patch-master software (HEKA, Lambrecht/Pfalz, Germany). Patch electrodes with a resistance of 4 MΩ to 6 MΩ were pulled from borosilicate glass capillaries using a micropipette puller (P-97 Sutter Instruments, Novato, CA). Liquid junction potentials were calculated with the algorithm developed by P.H. Burry [38] using Patch-master software and subtracted post acquisition. Seals (1 GΩ~10 GΩ) between the electrode and the cell were established. After whole cell configuration was established, the cell membrane capacitance and series resistance were electronically compensated. Series resistance was compensated 60% to 80%. In this study, small/medium sized DRG neurons, which were tested for AP and I_M, were defined by their membrane capacitance (≤ 35 pF). RTG (Selleckchem, Houston, TX) and XE991 (Sigma, St. Louis, MO) were dissolved in dimethyl Sulfoxide (DMSO) at 1,000 times of the final concentration and were kept frozen in aliquots. The stock solutions were diluted in the appropriate external solution just before use and delivered by PM 200B 4-Channel Pressure injector (Microdata Instrument, NJ). The distance from the column mouth to the cell studied was about 100 μm. The exposure time for RTG and XE991 was 2 minutes. It was demonstrated to be at steady-state phase by our preliminary experiments.

For voltage-clamp recording, the pipette solution contained (in mmol/L): 80 K-acetate, 30 KCl, 40 HEPES, 3 EGTA, 1 CaCl₂, 3 MgCl₂ and was adjusted to pH 7.4 by KOH. The external solution contained (in mmol/L): 144 NaCl, 2.5 KCl, 2 CaCl₂, 0.5 MgCl₂, 5 HEPES, 10 glucose and was adjusted to pH 7.4 by NaOH. In our experiments, K-acetate was used instead of high concentration of KCl in the pipette solution to reduce calcium-mediated rundown of I_Ms, because intracellular high KCl-induced outward chloride flux may lead to great inward calcium flux [39]. I_M was evoked by holding the membrane potential at -20 mV for 1 second and applying 1 second -50 mV repolarizing pulse. The amplitude of I_M was assessed by taking the difference of the

means between the initial (10 ms segment) and final of the repolarizing pulse. The I_M density was expressed as the ratio of the amplitude to membrane capacitance.

For current-clamp recording, the pipette solution contained (in mmol/L): 140 KCl, 4 NaCl, 10 HEPES, 10 EGTA, 0.5CaCl₂, 1 MgCl₂ and was adjusted to pH 7.4 by KOH. The external solution contained (in mmol/L): 140 NaCl, 5 KCl, 1.8 CaCl₂, 1 MgCl₂, 10 HEPES, 10 glucose and was adjusted to pH 7.4 by NaOH. Zero current was injected so that the neurons were held at their resting potential. The AP threshold was measured by a series of 5 ms depolarizing current injection in 10 pA steps from 0 pA to elicit the first AP. A depolarizing current pulse (1 second, 2 fold AP threshold) was delivered to elicit the cell generating sufficient firing and the frequency of AP was counted.

Animal groups and intragastric drug administration

Eight weeks after STZ injection, fifteen diabetic neuropathic pain rats were randomly divided into 3 groups (5 rats in each group) and were treated with PBS (2 ml), the KCNQ2/3/5 channels opener (RTG 5mg/kg), or the KCNQ2/3/5 channels blocker (XE991 5 mg/kg), respectively. Another fifteen age-matched normal rats were randomly divided into 3 groups (5 rats in each group) and were treated with PBS (2 ml), RTG (5mg/kg), or XE991 (5 mg/kg), respectively. All the drugs were dissolved in DMSO at 1,000 times of the final concentration and were kept frozen in aliquots. The drugs in the stock solutions were diluted by 2 ml PBS just before use and were given by a gastric tube inserted to the stomach of the rat by an injector. All the rats were tested for mechanical allodynia and thermal threshold every 30 minutes after drug administration. The mechanical allodynia and thermal hyperalgesia behavior tests were finished by the investigators who were blinded to the animal groups.

Evaluation of mechanical allodynia and thermal hyperalgesia

The threshold responses of the left and right hind paws to mechanical and thermal stimuli were detected by von Frey filaments (BME-403, Chinese Academy of Medical Sciences Institute of Biomedical Engineering) and a plantar analgesia tester (BME-400C, Chinese academy of medical sciences institute of biomedical engineering). All the rats received training sessions before behavioral tests.

Mechanical hypersensitivity was judged by the 50% withdrawal threshold to the relative stimulation. The rats used for mechanical allodynia test were adapted to the environment for 1 hour in a clear plastic cage with a wire mesh bottom that allowed full access to the rat hind paw. A series of standard von Frey filaments were used in series to stimulate the intermediate region on the plantar surface of the rat hind paw. The rats were given a pressure that was just adequate to bend the filament for 5 seconds. A positive response was considered as a brisk withdrawal of the testing hind paw. The 50% threshold was calculated according to the sequence of positive and negative scores as previously described [40].

The withdrawal latency to noxious radiant heat stimulation was used to evaluate the thermal hyperalgesia. Each rat for thermal hyperalgesia assessment was adapted to the environment for 1 hour and then was placed on a thin glass platform maintained at 30°C. A radiant heat source with constant intensity was used to stimulate the plantar intermediate region of the rat hind paw. The withdrawal latency was determined from the beginning of thermal stimulation until a brisk withdrawal of the hind paw. A cutoff of 30 seconds was used to prevent hind paw from tissue injury.

Statistical analysis

All the data was processed for verifying normality test. If normality test failed, the data were analyzed with non-parametric test. If normality test is passed, the Student's *t*-test was used to compare the differences between two groups by SPSS (version 15.0) software. *AP* value < 0.05 was delineated to be significant for analysis of all results.

Results

KCNQ2/3/5 channels mRNA expression in DRG of diabetic rats

Neuropathic injury induces a large-scale remodelling of nociceptive neurons driven by long-term changes in gene expression [41]. Whether diabetic mechanical allodynia and thermal hyperalgesia induced by diabetic neuropathy is associated with downregulation of KCNQ2/3/5 channels should be explored. Since KCNQ2/3/5 channels do not express in glia cells of DRG, the expression of KCNQ2/3/5 channels in the whole DRG tissue could reflect changes of KCNQ2/3/5 channels in DRG neurons [8]. Real-time PCR analysis revealed that the Δ Ct values of KCNQ2/3/5 channels

increased significantly in DRG of diabetic neuropathic pain rats, suggesting the downregulation of KCNQ2/3/5 channels is associated with mechanical allodynia and thermal hyperalgesia in diabetic neuropathic pain rats (Fig. 1).

KCNQ2/3/5 channels protein expression in DRG of diabetic rats

The decrease of mRNA levels of KCNQ2/3/5 channels in diabetic neuropathic pain rats suggested the KCNQ2/3/5 channels were down-regulated in transcription level. Western blot assay was performed to determine the protein levels of KCNQ2/3/5 channels in DRGs of diabetic neuropathic pain rats. Similar to the mRNA of KCNQ2/3/5 channels, the protein levels of KCNQ2/3/5 channels also decreased in DRG from diabetic rats (Fig. 2).

KCNQ2/3/5 channels expression in situ in DRG neurons of diabetic rats

We further detected the changes of KCNQ2/3/5 channels expression in situ in DRG neurons by double fluorescent labeling. KCNQ2/3/5 channels (red) were co-localized with the neuron marker MAP2 (green) and nociceptive neuron marker TRPV1 (green) in the present study. Consistent with our real-time PCR and Western blot data, the proportion of KCNQ2/3/5-positive neurons (red) to the MAP2-positive neurons (green) decreased significantly in DRG from diabetic rats. In addition, the immunofluorescence intensity of KCNQ2/3/5 channels of diabetic rats was weaker than that in the control group (Fig. 3). Double fluorescent labeling of KCNQ2/3/5 and TRPV1 revealed that the proportion of the TRPV1 co-localized neurons (orange) to the KCNQ2/3/5-positive neurons (red) increased in DRG from diabetic neuropathic pain rats (Fig. 4).

I_M density of DRG neurons and drug influence

Voltage-clamp recordings were used to assess the effects of diabetic neuropathic pain on I_M density of DRG neurons, which were small and medium sized DRG neurons with their membrane capacitance (≤ 35 pF). Compared with normal control rats, the I_M density of DRG neurons in diabetic rats reduced significantly, which might be the result of decreased expression of KCNQ2/3/5 channels. The KCNQ2/3/5 channel opener RTG (10 $\mu\text{mol/L}$) treatment significantly enhanced I_M density of DRG neurons in diabetic rats and in non-diabetic control rats. The KCNQ2/3/5 channel blocker XE991 (1 $\mu\text{mol/L}$) treatment reduced I_M density of DRG neurons in

both diabetic rats and normal control rats. Moreover, RTG and XE991 had more predominant effects on I_M density of DRG neurons in control rats than diabetic rats (Fig. 5).

Excitability of DRG neurons and drug influence

We used current-clamp recordings of cultured DRG neurons from rats with or without diabetic neuropathic pain to characterize the changes of sensory neuronal excitability. The small and medium sized DRG neurons from diabetic rats exhibited dramatically enhanced neuronal excitability, including depolarized RMP, reduction in AP threshold, and increase in frequency of AP. RTG (10 $\mu\text{mol/L}$) could inhibit neuronal excitability manifested as hyperpolarized RMP, increase in AP threshold, and decrease in frequency of AP of small and medium sized DRG neurons from diabetic and normal control rats. XE991 (1 $\mu\text{mol/L}$) enhanced neuronal excitability by the same way in both diabetic and normal control rats (Fig. 6).

Mechanical allodynia and thermal hyperalgesia and drug influence

Rats with STZ-induced diabetes showed hypersensitivity to noxious mechanical and thermal stimulation, as previously described by other studies [42, 43]. Our preliminary experiment demonstrated that intragastric administration of RTG to diabetic rats and control rats affected mechanical and thermal thresholds in a time dependent manner, and the peak of effect was at 2 hours after administration. RTG increased paw withdrawal threshold to mechanical stimulation and extend withdrawal latency to thermal stimulation, while XE991 decreased paw withdrawal threshold to mechanical stimulation and shorten withdrawal latency to thermal stimulation of diabetic rats and control rats, suggesting KCNQ2/3/5 channels are potential targets for treatment of diabetic neuropathic pain (Fig. 7).

Discussion

Painful diabetic peripheral neuropathy is prevalent among diabetic patients and is increasing over time worldwide. However, the precise molecular mechanisms underlying hyperalgesia in diabetic neuropathy remain poorly understood, and effective treatment for this metabolic pain is limited. To explore the mechanism of diabetic neuropathic pain progression and to pursue new pharmacological targets are essential for finding new effective therapeutic strategy on relieving

diabetic neuropathic pain. In this work, a significant decrease of KCNQ2/3/5 channels in DRG from diabetic rats was detected. Additionally, KCNQ2/3/5 channels in the DRG neurons of diabetic neuropathic rats were distributed along with TRPV1-positive nociceptive sensory neurons, which were activated in diabetic neuropathy-induced hyperalgesia [44]. The I_M density of DRG neurons in diabetic rats significantly reduced, in agreement with significant decline of expression of KCNQ2/3/5 channels in DRG from diabetic rats. The KCNQ2/3/5 channel opener RTG increased I_M density and inhibited neuronal excitability of DRG neurons from diabetic rats, whereas the KCNQ2/3/5 channel blocker XE991 had the opposite effects. In electrophysiological recordings of diabetic neuropathic DRG neurons, the effects of RTG and XE991 were less sensitive than the control group because their target KCNQ2/3/5 channels' expression was decreased during the development of diabetic neuropathy. RTG also attenuated responses to mechanical allodynia and thermal hyperalgesia of diabetic neuropathic rats in a time dependent manner with the peak of effect at 2 hours after administration. On the other hand, the KCNQ2/3/5 blocker XE991 potentiated the responses of mechanical allodynia and thermal hyperalgesia in diabetic neuropathic rats. The results of our present study show that KCNQ2/3/5 channels expressed in the DRG neurons contribute to the development of mechanical allodynia and thermal hyperalgesia in diabetic neuropathy. Targeting the peripherally distributed KCNQ2/3/5 channels in DRG neurons may represent a viable therapeutic strategy for the treatment of diabetic neuropathic pain.

KCNQ channels are voltage-dependent potassium channels composed of combinations of subunits, being differently expressed in the DRG neurons. Some DRG neurons expressed both KCNQ2 and KCNQ3, while others expressed KCNQ2 in the absence of KCNQ3. Likewise, although some cells expressed both KCNQ3 and KCNQ5, others expressed KCNQ3 in the absence of KCNQ5 [45]. Notably, the expression KCNQ2/3/5 channels are significantly suppressed by the development of diabetic neuropathy. The role of KCNQ channel opener RTG and KCNQ channel blocker XE991 in the involvement of diabetic neuropathic pain on the down-regulated expressed KCNQ2/3/5 channels should be resolved. We therefore assessed the effect of RTG and XE991 on KCNQ2/3/5 channels both in vivo and in vitro experiments. Diabetic neuropathy caused a marked reduction in the number of KCNQ-expression neurons and induced a strong excitatory status of sensory neuron, which suggested that KCNQ channels play a direct role in regulating sensory

excitability *in vivo*. The administration of RTG and XE991 in the rat also targeted KCNQ and affected neuropathic pain behavior. But the mechanism of KCNQ should be further confirmed by *in vitro* experiments.

The I_M is a voltage-dependent, persistent K^+ current that is strongly regulated. The main function of I_M is to limit neuronal excitability by contrasting AP firing [35]. The *in situ* expression of KCNQ2/3/5 channels in the diabetic rat DRG slice is decreased. On this condition, we employed the whole-cell patch-clamp technique to record DRG neuronal AP and I_M using an *in vitro* model of DRG neuronal culture. I_M evoked in voltage-clamp experiments demonstrated that density of I_M was significantly reduced in DRG neurons of diabetic rats. AP, which was strongly regulated by I_M , was measured in current-clamp recording. Accordingly, the reduced density of I_M had apparently resulted in depolarized RMP, reduction in AP threshold, and increase in frequency of AP in the small and medium sized DRG neurons of diabetic rats. Our results suggest that DRG neurons possess I_M , which is importantly down-regulated in diabetic neuropathic rats and failed to modulate the excitability of afferent neurons. The pharmacological activities of I_M opener and blocker were also explored in our experimental models of diabetic neuropathy.

RTG were used in both *in vitro* models to provide a better understanding of the electrophysiology of neurons, and allow for the treatment of the neuropathic pain in animal models [3, 34]. With patch-clamp recording, we investigated the changes of density of I_M of small/medium sized DRG neurons pretreated with RTG and different effect of RTG to provoke I_M when expression of KCNQ2/3/5 channels was down-regulated by diabetic neuropathy. Although RTG treatment significantly enhanced I_M density of DRG neurons in diabetic rats and in non-diabetic control rats, it had less effect on DRG neurons from diabetic rats due to down-regulated expression of KCNQ2/3/5 channels. But RTG are still potent on reducing the pathological excitability of DRG neurons of diabetic neuropathic rats, which is also reflected by *in vivo* study that RTG reduced mechanical allodynia and thermal hyperalgesia of diabetic neuropathic rats.

XE991, which is being used increasingly in experiments, is a compound that specifically targets the activated subunit of KCNQ channels [37]. Here, we demonstrated the inhibiting effect of XE991 on KCNQ channels both in patch-clamp experiments and in animal experiments. The result showed that the effects of XE991 were practically opposite of RTG, including reduced I_M density and enhanced neuronal excitability of DRG neurons by depolarizing RMP, reducing AP

threshold, and increasing in frequency of AP. The patch-clamp experiments were performed on DRG neurons from diabetic neuropathic rats whose expression of KCNQ channels was down-regulated. A recent study showed that XE991 is a state-dependent inhibitor that favors the activated single subunit of neuronal KCNQ channels [37]. In our present experiment, when the expression of KCNQ2/3/5 channels was decreased, the effectiveness potential for XE991 to inhibit I_M of DRG neurons was not as sensitive as the normal control. This result suggested that DRG neurons of diabetic neuropathic rats could not provide sufficient KCNQ2/3/5 channel subunits to transport to the cell surface to meet physiologic conditions.

Both RTG and XE991 were state-dependent drugs that were less efficacious when expression of KCNQ2/3/5 channels was decreased during diabetic neuropathy. Pharmacological effects of RTG and XE991 were sensitive to changes of expression of KCNQ channels. The electrophysiological changes of DRG neurons by RTG or XE991 treatment could well explain the changes of KCNQ2/3/5 channels on DRG neurons of diabetic neuropathic rats. KCNQ2/3/5 channels are likely to be implicated in the nociceptive sensory transduction of diabetic neuropathic pain. Concerning the heterogeneity of DRG neurons of different subpopulations, tyrosine kinase receptor (Trk)A-positive neurons represent the peptidergic nociceptors which are mainly small sized DRG neurons for pain and nociception signaling transmission. These subpopulations are largely overlapped with TRPV1 expressing peptidergic neurons. TrkB-positive neurons represent the mechanoreceptors which vary from small to large cells. TrkC-positive neurons represent proprioceptors which are mainly large cells with myelinated axons. These three subsets (TrkA, TrkB, and TrkC) are restricted to subtypes of mature DRG neurons with only minimally overlap [46-49]. According to the category of DRG neurons, the small/medium sized DRG neurons are mainly responsible for the pain-related signaling transmission. This point was used in the electrophysiological recordings for analyzing isolated living DRG neurons in our present study. Hence, the recorded neurons in the electrophysiological experiment were defined as small/medium sized DRG neurons with their membrane capacitance ≤ 35 pF, despite the fact that their sensory modality could not be detected directly. This is one of the limitations in our work.

Although targeting KCNQ2/3/5 channels in DRG neurons is a promising novel approach for relieving diabetic neuropathic pain as shown in our present study, the central mechanism also needs to be explored because of the central sensitization induced indirectly by peripheral

nociceptive signaling transmission or directly by high glucose challenges. Upregulation of inflammatory cytokines [50], alteration of proinflammatory neuropeptides [51] and N-methyl-D-aspartate (NMDA) receptor phosphorylation in spinal dorsal horn [29], activation of anterior cingulate cortex [28], and brain-based facilitatory pain mechanism [52] contribute to diabetic neuropathic pain. Combined peripheral and central targeting approach may represent the potential strategy on relieving diabetic neuropathic pain in future.

In conclusion, the findings elucidate the mechanisms by which downregulation of expression and activities of KCNQ2/3/5 channels in diabetic rat DRG neurons contributes to their enhanced neuronal excitability which results in mechanical allodynia and thermal hyperalgesia and provide intriguing evidence that activation of KCNQ2/3/5 channels might be the potential new targets for alleviating diabetic neuropathic pain symptoms. To further confirm the pain relieving efficiency by targeting KCNQ2/3/5 channels in diabetic patients as new therapy strategy is anticipated.

Authors' contributions

TY, HL, and ZL conceived the study. TY, LL, HL, and ZL obtained diabetic animals and carried out behavior testing, PCR, Western blot assay, and fluorescence labeling. TY performed electrophysiological experiments. TY, ZL, and ZL contributed to the analysis and interpretation of the data. TY and ZL wrote the manuscript. All authors have substantially contributed to the revision of the manuscript, have read and approved the final version.

Acknowledgements

We thank Miss Jingyi Huang, who is from the University of Toronto Human Biology Program, for her careful revision of this version of our manuscript.

Declaration of conflicting interests

The author(s) declared no potential conflicts of interest with respect to the research, authorship, and/or publication of this article.

Funding

The author(s) disclosed receipt of the following financial support for the research, authorship, and/or publication of this article: This work was supported by the National Natural Science Foundation of China (No. 81371929), the Shandong Provincial Natural Science Foundation of China (No. ZR2014HL038), and the Science and Technology Boost New Energy Conversion Plan in Jining (No. 2017 MNS004).

References

1. Wang JJ, Li Y. KCNQ potassium channels in sensory system and neural circuits. *Acta Pharmacol Sin.* 2016;37(1):25-33.
2. Hansen HH, Weikop P, Mikkelsen MD, Rode F, Mikkelsen JD. The pan-Kv7 (KCNQ) Channel Opener Retigabine Inhibits Striatal Excitability by Direct Action on Striatal Neurons In Vivo. *Basic Clin Pharmacol Toxicol.* 2017;120(1):46-51.
3. Peiris M, Hockley JR, Reed DE, Smith ESJ, Bulmer DC, Blackshaw LA. Peripheral KV7 channels regulate visceral sensory function in mouse and human colon. *Mol Pain.* 2017;13:1744806917709371.
4. Berg T. Kv7(KCNQ)-K⁺-channels influence total peripheral resistance in female but not male rats, and hamper catecholamine release in hypertensive rats of both sexes. *Front Physiol.* 2018;9:117.
5. Chang A, Abderemane-Ali F, Hura GL, Rossen ND, Gate RE, Minor DL Jr. A calmodulin C-lobe Ca²⁺-dependent switch governs Kv7 channel function. *Neuron.* 2018;97(4):836-852.
6. Barrese V, Stott JB, Greenwood IA. KCNQ-encoded potassium channels as therapeutic targets. *Annu Rev Pharmacol Toxicol.* 2018;58:625-648.
7. Lombardo J, Sun J, Harrington MA: Rapid activity-dependent modulation of the intrinsic excitability through up-regulation of KCNQ/Kv7 channel function in neonatal spinal motoneurons. *PLoS One.* 2018;13(3):e0193948.
8. Miceli F, Soldovieri MV, Ambrosino P, Manocchio L, Medoro A, Mosca I, et al. Pharmacological targeting of neuronal Kv7.2/3 channels: A focus on chemotypes and receptor sites. *Curr Med Chem.* 2017;Oct 12. [Epub ahead of print]

9. Teng BC, Song Y, Zhang F, Ma TY, Qi JL, Zhang HL, et al. Activation of neuronal Kv7/KCNQ/M-channels by the opener QO58-lysine and its anti-nociceptive effects on inflammatory pain in rodents. *Acta Pharmacol Sin.* 2016;37(8):1054-1062.
10. Wu Z, Li L, Xie F, Du J, Zuo Y, Frost JA, et al. Activation of KCNQ channels suppresses spontaneous activity in dorsal root ganglion neurons and reduces chronic pain after spinal cord injury. *J Neurotrauma.* 2017;34(6):1260-1270.
11. Greene DL, Hoshi N. Modulation of Kv7 channels and excitability in the brain. *Cell Mol Life Sci.* 2017;74(3):495-508.
12. Lombardo J, Harrington MA. Nonreciprocal mechanisms in up- and downregulation of spinal motoneuron excitability by modulators of KCNQ/Kv7 channels. *J Neurophysiol.* 2016;116(5):2114-2124.
13. Zwart R, Reed H, Clarke S, Sher E. A novel muscarinic receptor-independent mechanism of KCNQ2/3 potassium channel blockade by Oxotremorine-M. *Eur J Pharmacol.* 2016;791:221-228.
14. Abd-Elsayed AA, Ikeda R, Jia Z, Ling J, Zuo X, Li M, et al. KCNQ channels in nociceptive cold-sensing trigeminal ganglion neurons as therapeutic targets for treating orofacial cold hyperalgesia. *Mol Pain.* 2015;11:45.
15. Paisley P, Serpell M. Improving pain control in diabetic neuropathy. *Practitioner.* 2017;261(1802):23-26.
16. Stino AM, Smith AG. Peripheral neuropathy in prediabetes and the metabolic syndrome. *J Diabetes Investig.* 2017;8(5):646-655.
17. Chen T, Li H, Yin Y, Zhang Y, Liu Z, Liu H. Interactions of Notch1 and TLR4 signaling pathways in DRG neurons of in vivo and in vitro models of diabetic neuropathy. *Sci Rep.* 2017;7(1):14923.
18. Miranda HF, Sierralta F, Jorquera V, Poblete P, Prieto JC, Noriega V. Antinociceptive interaction of gabapentin with minocycline in murine diabetic neuropathy. *Inflammopharmacology.* 2017;25(1):91-97.
19. Nicodemus JM, Enriquez C, Marquez A, Anaya CJ, Jolivald CG. Murine model and mechanisms of treatment-induced painful diabetic neuropathy. *Neuroscience.* 2017;354:136-145.

20. Zhu GC, Tsai KL, Chen YW, Hung CH. Neural mobilization attenuates mechanical allodynia and decreases proinflammatory cytokine concentrations in rats with painful diabetic neuropathy. *Phys Ther.* 2018;98(4):214-222.
21. Gilron I, Tu D, Holden R, Jackson AC, Ghasemlou N, Duggan S, et al. Pain improvement with novel combination analgesic regimens (PAIN-CARE): Randomized controlled trial protocol. *JMIR Res Protoc.* 2017;6(6):e111.1
22. Lu Y, Lin B, Zhong J. The therapeutic effect of dexmedetomidine on rat diabetic neuropathy pain and the mechanism. *Biol Pharm Bull.* 2017;40(9):1432-1438.
23. Waldfoegel JM, Nesbit SA, Dy SM, Sharma R, Zhang A, Wilson LM, et al. Pharmacotherapy for diabetic peripheral neuropathy pain and quality of life: A systematic review. *Neurology.* 2017;88(20):1958-1967.
24. Zeng L, Alongkronrusmee D, van Rijn RM. An integrated perspective on diabetic, alcoholic, and drug-induced neuropathy, etiology, and treatment in the US. *J Pain Res.* 2017;10:219-228.
25. Zilliox LA. Neuropathic Pain. *Continuum (Minneapolis, Minn).* 2017;23(2, Selected Topics in Outpatient Neurology):512-532.
26. van Beek M, van Kleef M, Linderoth B, van Kuijk SM, Honig WM, Joosten EA. Spinal cord stimulation in experimental chronic painful diabetic polyneuropathy: Delayed effect of High-frequency stimulation. *Eur J Pain.* 2017;21(5):795-803.
27. Kumar A, Kaur H, Singh A. Neuropathic Pain models caused by damage to central or peripheral nervous system. *Pharmacol Rep.* 2018;70(2):206-216.
28. Watanabe K, Hirano S, Kojima K, Nagashima K, Mukai H, Sato T, et al. Altered cerebral blood flow in the anterior cingulate cortex is associated with neuropathic pain. *J Neurol Neurosurg Psychiatry.* 2018;Apr 7. [Epub ahead of print]
29. Zhao JY, Yang L, Bai HH, Liu JP, Suo ZW, Yang X, et al. Inhibition of protein tyrosine phosphatase 1B in spinal cord dorsal horn of rats attenuated diabetic neuropathic pain. *Eur J Pharmacol.* 2018;827:189-197.
30. Jayaraj ND, Bhattacharyya BJ, Belmadani AA, Ren D, Rathwell CA, Hackelberg S, et al. Reducing CXCR4-mediated nociceptor hyperexcitability reverses painful diabetic neuropathy. *J Clin Invest.* 2018;128:2205-2225.

31. Eldabe S, Espinet A, Wahlstedt A, Kang P, Liem L, Patel NK, et al. Retrospective case series on the treatment of painful diabetic peripheral neuropathy with dorsal root ganglion stimulation. *Neuromodulation*. 2018;Mar 25. [Epub ahead of print]
32. Hayashi H, Iwata M, Tsuchimori N, Matsumoto T. Activation of peripheral KCNQ channels attenuates inflammatory pain. *Mol Pain*. 2014;10(1):15.
33. Zhou N, Huang S, Li L, Huang D, Yan Y, Du X, et al. Suppression of KV7/KCNQ potassium channel enhances neuronal differentiation of PC12 cells. *Neuroscience*. 2016;333:356-367.
34. Aizawa N, Wakamatsu D, Kida J, Otsuki T, Saito Y, Matsuya H, et al. Inhibitory effects of retigabine, a Kv7 channel activator, on mechanosensitive primary bladder afferent activities and nociceptive behaviors in rats. *NeuroUrol Urodyn*. 2017;36(2):280-285.
35. Ghezzi F, Corsini S, Nistri A. Electrophysiological characterization of the M-current in rat hypoglossal motoneurons. *Neuroscience*. 2017;340:62-75.
36. Kuo FS, Falquetto B, Chen D, Oliveira LM, Takakura AC, Mulkey DK. In vitro characterization of noradrenergic modulation of chemosensitive neurons in the retrotrapezoid nucleus. *J Neurophysiol*. 2016;116(3):1024-1035.
37. Greene DL, Kang S, Hoshi N. XE991 and linopirdine are state-dependent inhibitors for Kv7/KCNQ channels that favor activated single subunits. *J Pharmacol Exp Ther*. 2017;362(1):177-185.
38. Barry PH. JPCalc, a software package for calculating liquid junction potential corrections in patch-clamp, intracellular, epithelial and bilayer measurements and for correcting junction potential measurements. *J Neurosci Methods*. 1994;51(1):107-116.
39. Vernino S, Amador M, Luetje CW, Patrick J, Dani JA. Calcium modulation and high calcium permeability of neuronal nicotinic acetylcholine receptors. *Neuron*. 1992;8(1):127-134.
40. Lolignier S, Eijkelkamp N, Wood JN. Mechanical allodynia. *Pflugers Arch*. 2015;467(1):133-139.
41. Bierhaus A, Fleming T, Stoyanov S, Leffler A, Babes A, Neacsu C, et al. Methylglyoxal modification of Nav1.8 facilitates nociceptive neuron firing and causes hyperalgesia in diabetic neuropathy. *Nat Med*. 2012;18(6):926-933.
42. Kishore L, Kaur N, Singh R. Effect of Kaempferol isolated from seeds of *Eruca sativa* on changes of pain sensitivity in Streptozotocin-induced diabetic neuropathy.

- Inflammopharmacology. 2017;Nov 20. [Epub ahead of print]
43. Mittal R, Kumar A, Singh DP, Bishnoi M, Nag TC. Ameliorative potential of rutin in combination with nimesulide in STZ model of diabetic neuropathy: targeting Nrf2/HO-1/NF-kB and COX signalling pathway. *Inflammopharmacology*. 2018;26:755-768.
 44. Zan Y, Kuai CX, Qiu ZX, Huang F. Berberine ameliorates diabetic neuropathy. TRPV1 modulation by PKC pathway. *Am J Chin Med*. 2017;45:1709-1723.
 45. Passmore GM, Selyanko AA, Mistry M, Al-Qatari M, Marsh SJ, Matthews EA, et al. KCNQ/M currents in sensory neurons: significance for pain therapy. *J Neurosci*. 2003;23(18):7227-7236.
 46. Li H, Dong H, Li J, Liu H, Liu Z, Li Z. Neuroprotective effect of insulin-like growth factor-1: Effects on tyrosine kinase receptor (Trk) expression in dorsal root ganglion neurons with glutamate-induced excitotoxicity in vitro. *Brain Res Bull*. 2013;97C:86-95.
 47. Haddad Y, Adam V, Heger Z. Trk receptors and neurotrophin cross-interactions: New perspectives toward manipulating therapeutic side-effects. *Front Mol Neurosci*. 2017;10:130.
 48. Cheng I, Jin L, Rose LC, Deppmann CD. Temporally restricted death and the role of p75NTR as a survival receptor in the developing sensory nervous system. *Dev Neurobiol*. 2018;Mar 22. [Epub ahead of print]
 49. Skaper SD. Neurotrophic factors: An overview. *Methods Mol Biol*. 2018;1727:1-17.
 50. Yao L, Wu YT, Tian GX, Xia CQ, Zhang F, Zhang W. Acrolein scavenger hydralazine prevents streptozotocin-induced painful diabetic neuropathy and spinal neuroinflammation in rats. *Anat Rec (Hoboken)*. 2017;300(10):1858-1864.
 51. Wan FP, Bai Y, Kou ZZ, Zhang T, Li H, Wang YY, et al. Endomorphin-2 inhibition of substance P signaling within lamina I of the spinal cord is impaired in diabetic neuropathic pain rats. *Front Mol Neurosci*. 2017;9:167.
 52. Segerdahl AR, Themistocleous AC, Fido D, Bennett DL, Tracey I. A brain-based pain facilitation mechanism contributes to painful diabetic polyneuropathy. *Brain*. 2018;141(2):357-364.

Fig. 1. Expression of mRNA for KCNQ2/3/5 channels in DRG. The relative expression ratio of KCNQ2/3/5 channels significantly decreased in DRG of diabetic neuropathic pain rats. Bar graphs represent mean \pm SEM, n=5, * P <0.01, paired Student's t -test.

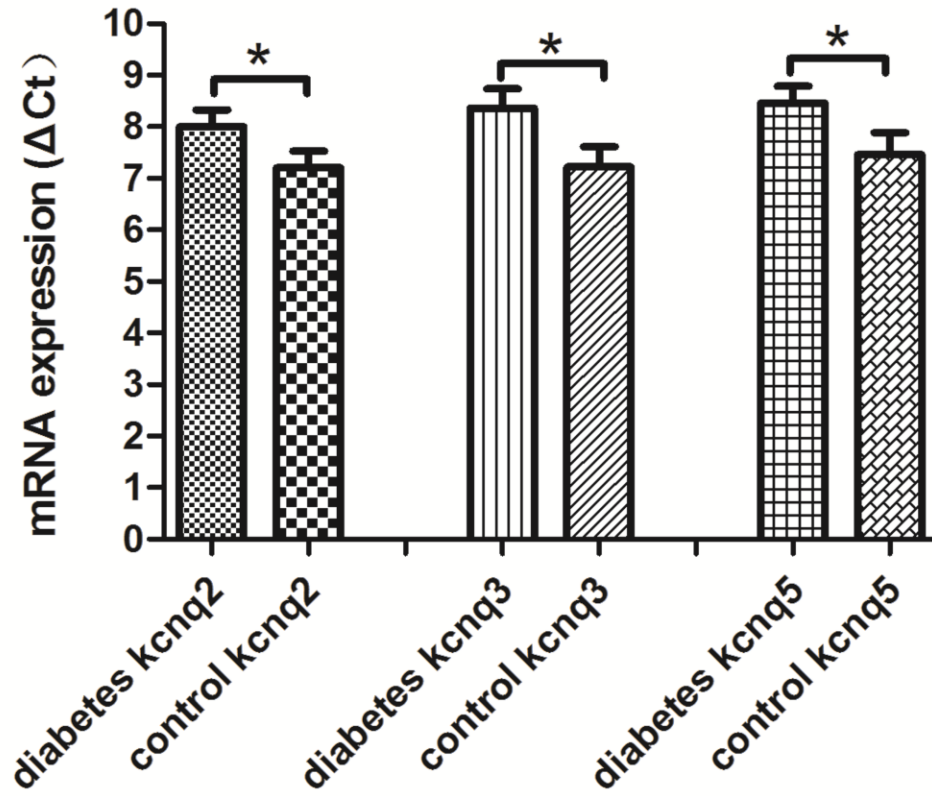


Fig. 2. Expression of KCNQ2/3/5 channels protein in DRG. Western blot assay exhibited the downregulation of KCNQ2 (A1, A2), KCNQ3 (B1, B2) and KCNQ5 (C1, C2) protein levels in DRG of diabetic neuropathic pain rats in contrast to normal control rats. The lysates represented in panels A1/2/3 were from the same control animals and diabetic animals, respectively. Bar graphs with error bars represent mean \pm SEM, $n=5$, * $P<0.05$, ** $P<0.01$, paired Student's t -test.

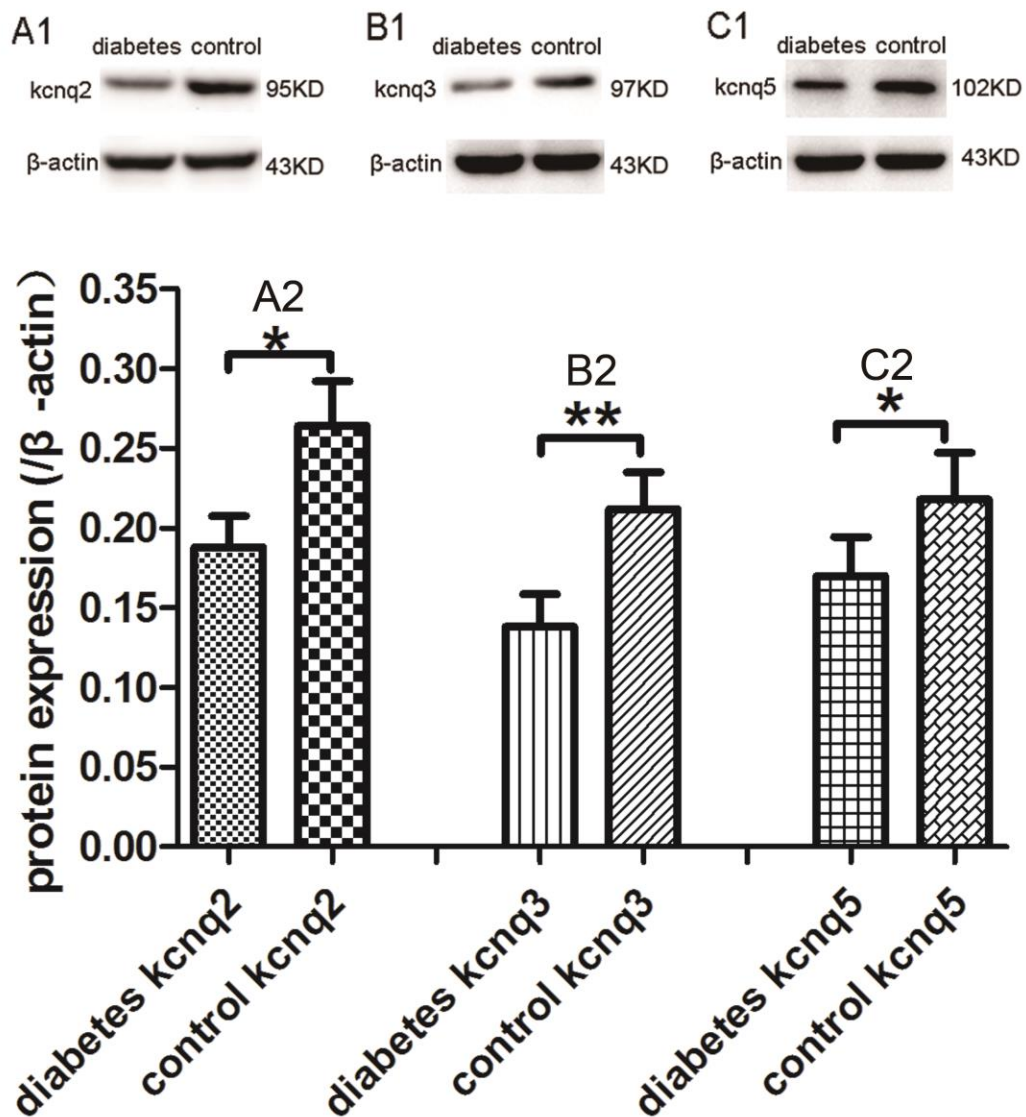


Fig. 3. KCNQ2/3/5 channels expression in situ in DRG neurons. Double fluorescent labeling revealed that the percentage of KCNQ2/3/5-positive neurons of total neurons (MAP2-positive neurons) decreased dramatically in DRG of diabetic neuropathic pain rats compared to normal control rats. (A1-A4) The examples of MAP2-positive (green), KCNQ2-positive (red) DRG neurons, overlay, and no-primary antibody control in diabetic rats. (B1-B4) The examples of MAP2-positive (green), KCNQ2-positive (red) DRG neurons, overlay, and no-primary antibody control in normal control rats. (C1-C4) The examples of MAP2-positive (green), KCNQ3-positive (red) DRG neurons, overlay, and no-primary antibody control in diabetic rats. (D1- D4) The examples of MAP2-positive (green), KCNQ3-positive (red) DRG neurons, overlay, and no-primary antibody control in normal control rats. (E1-E4) The examples of MAP2-positive (green), KCNQ5-positive (red) DRG neurons, overlay, and no-primary antibody control in diabetic rats. (F1-F4) The examples of MAP2-positive (green), KCNQ5-positive (red) DRG neurons, overlay, and no-primary antibody control in normal control rats. (G) The quantitative analysis of the proportion of KCNQ2/3/5-positive (red) to MAP2-positive (green) DRG neurons. (H) The quantitative analysis of KCNQ2/3/5 channels relative immunofluorescence intensity to MAP2 immunofluorescence intensity. Scale bar = 50 μ m. Bar graphs with error bars represent mean \pm SEM, n=5, * P <0.05, ** P <0.01, *** P <0.001, paired Student's *t*-test.

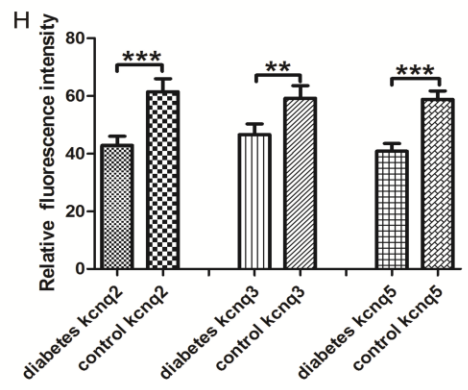
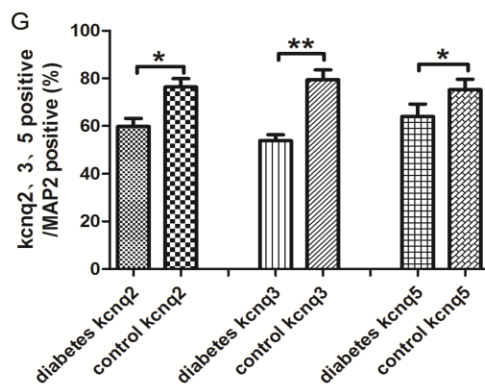
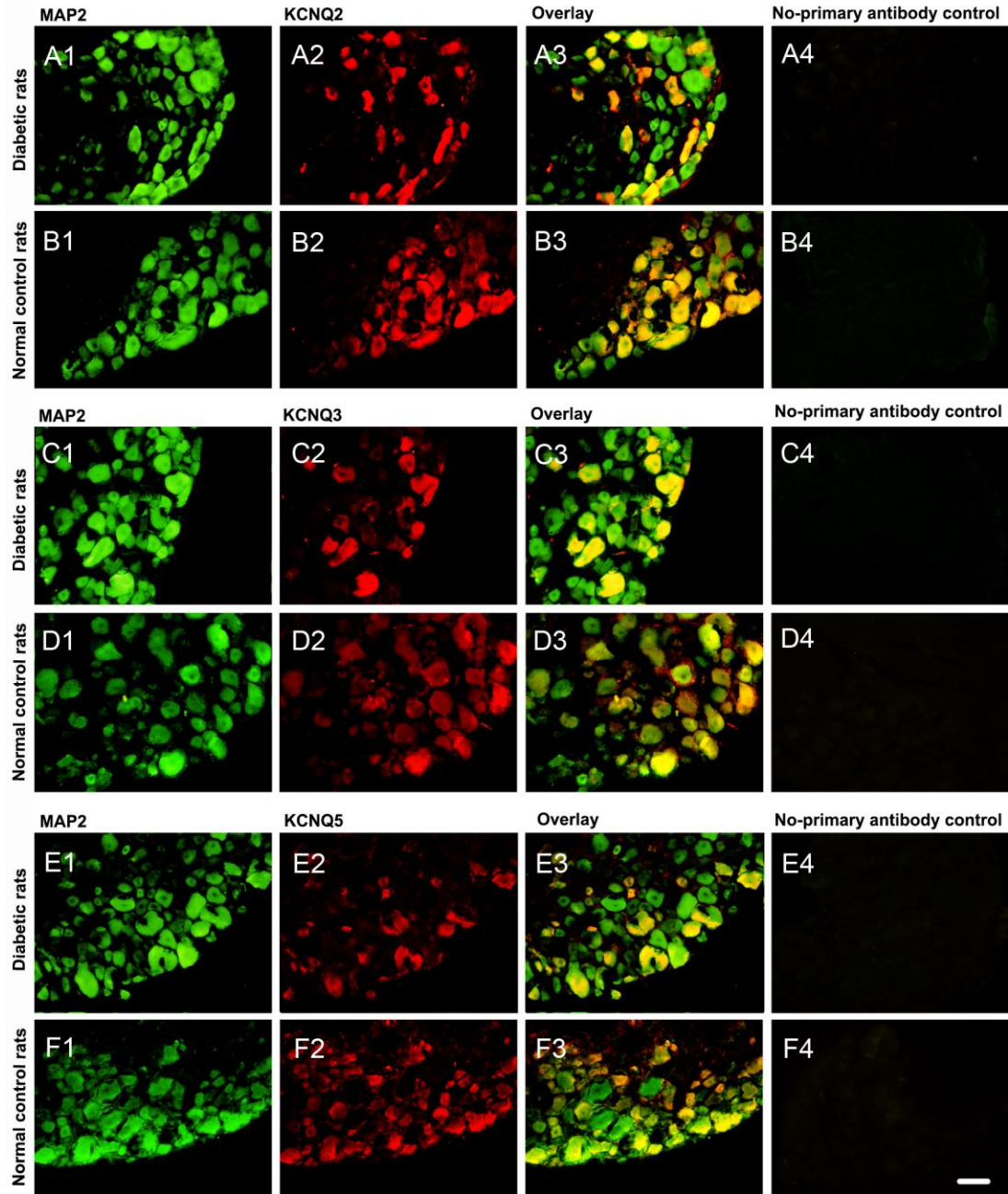


Fig. 4. Increased co-localization of TRPV1 and KCNQ2/3/5 in DRG neurons of neuropathic pain rats. (A1-A4) The examples of TRPV1-positive (green), KCNQ2-positive (red) DRG neurons, overlay, and no-primary antibody control in diabetic rats. (B1-B4) The examples of TRPV1-positive (green), KCNQ2-positive (red) DRG neurons, overlay, and no-primary antibody control in normal control rats. (C1-C4) The examples of TRPV1-positive (green), KCNQ3-positive (red) DRG neurons, overlay, and no-primary antibody control in diabetic rats. (D1- D4) The examples of TRPV1-positive (green), KCNQ3-positive (red) DRG neurons, overlay, and no-primary antibody control in normal control rats. (E1-E4) The examples of TRPV1-positive (green), KCNQ5-positive (red) DRG neurons, overlay, and no-primary antibody control in diabetic rats. (F1-F4) The examples of TRPV1-positive (green), KCNQ5-positive (red) DRG neurons, overlay, and no-primary antibody control in normal control rats. (G) The quantitative analysis of the proportion of TRPV1 co-localized neurons (orange) to KCNQ2/3/5-positive neurons (red). Scale bar = 50 μ m. Bar graphs with error bars represent mean \pm SEM, $n=5$, $*P < 0.01$, paired Student's *t*-test.

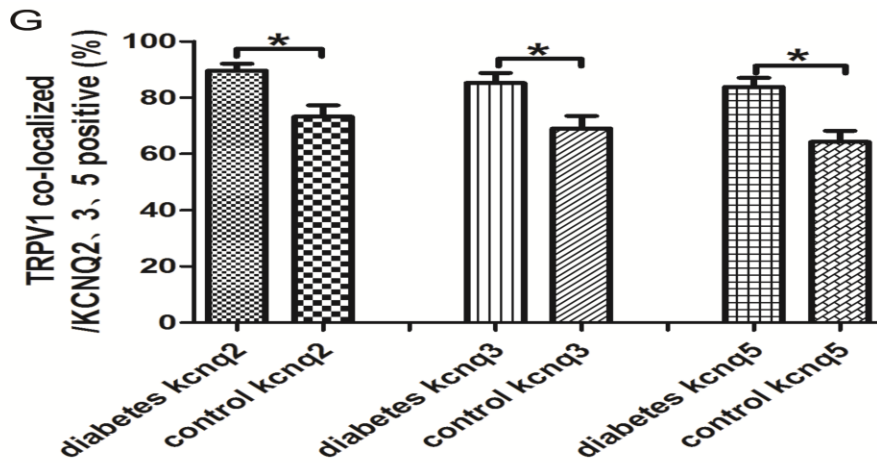
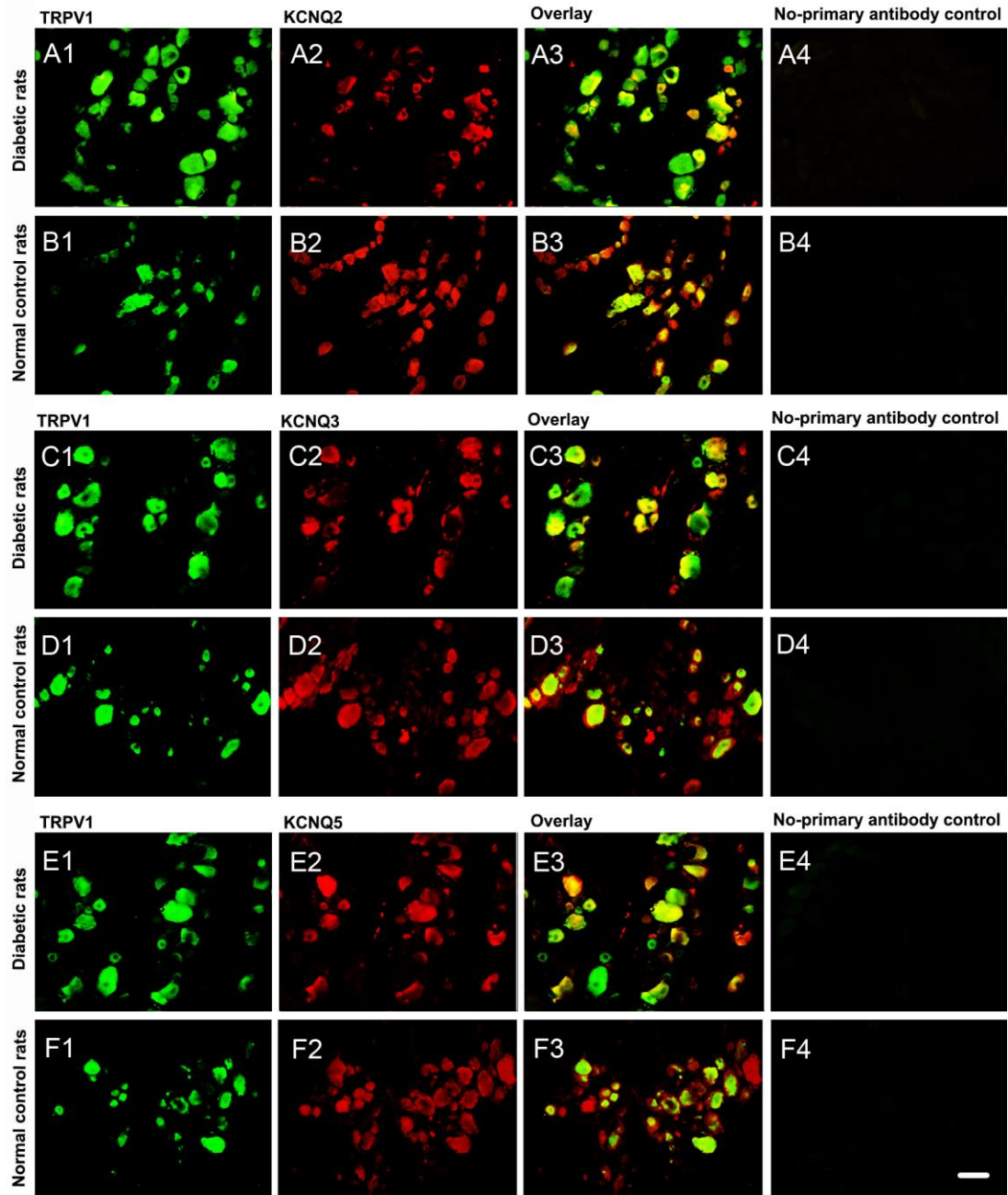


Fig. 5. M current of DRG neurons and drug influence. (A) Standard protocol for recording M current. (B) A representative example of M current recorded from a DRG neuron (33.4 pF) of diabetic neuropathic pain rats before (black) and after (red) perfusion with retigabine (10 $\mu\text{mol/L}$). (C) A representative example of M current recorded from a DRG neuron (22.3 pF) of diabetic neuropathic pain rats before (black) and after (red) perfusion with XE991 (1 $\mu\text{mol/L}$). (D) A representative example of M current recorded from a DRG neuron (28.4 pF) of normal control rat before (black) and after (red) perfusion with retigabine (10 $\mu\text{mol/L}$). (E) A representative example of M current recorded from a DRG neuron (19.8 pF) of normal control rat before (black) and after (red) perfusion with XE991 (1 $\mu\text{mol/L}$). (F) The quantitative analysis of M current density before and after perfusion with retigabine (10 $\mu\text{mol/L}$) or XE991 (1 $\mu\text{mol/L}$). Bar graphs with error bars represent mean \pm SEM, $n=40$, $*P<0.001$, diabetes vs control, unpaired Student's *t*-test, others paired Student's *t*-test.

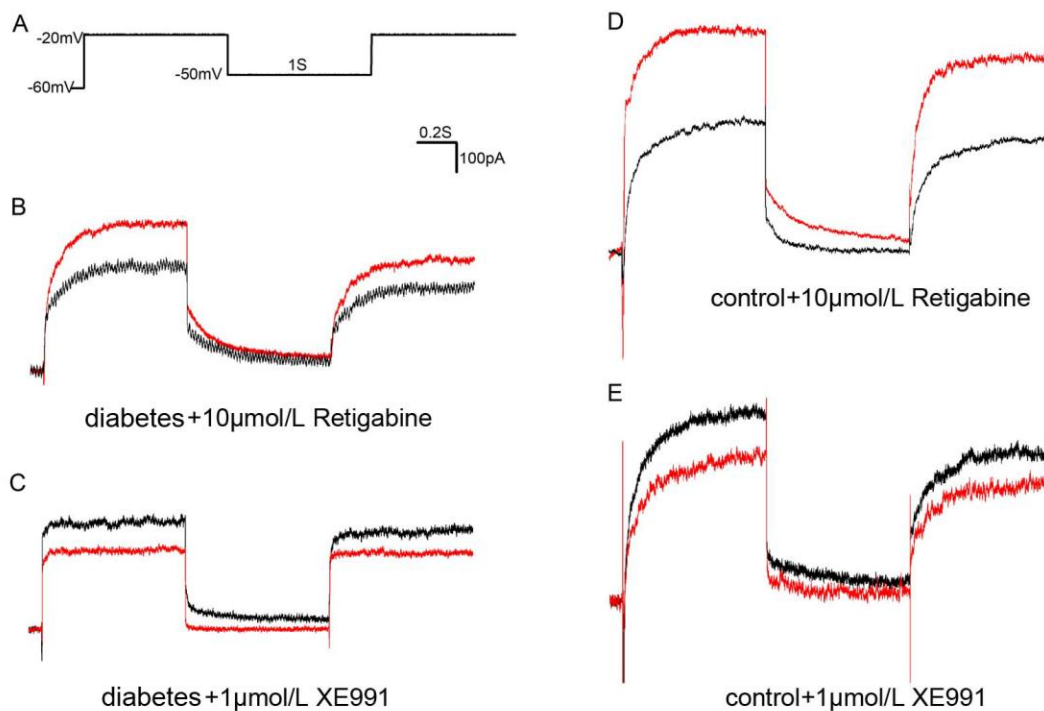
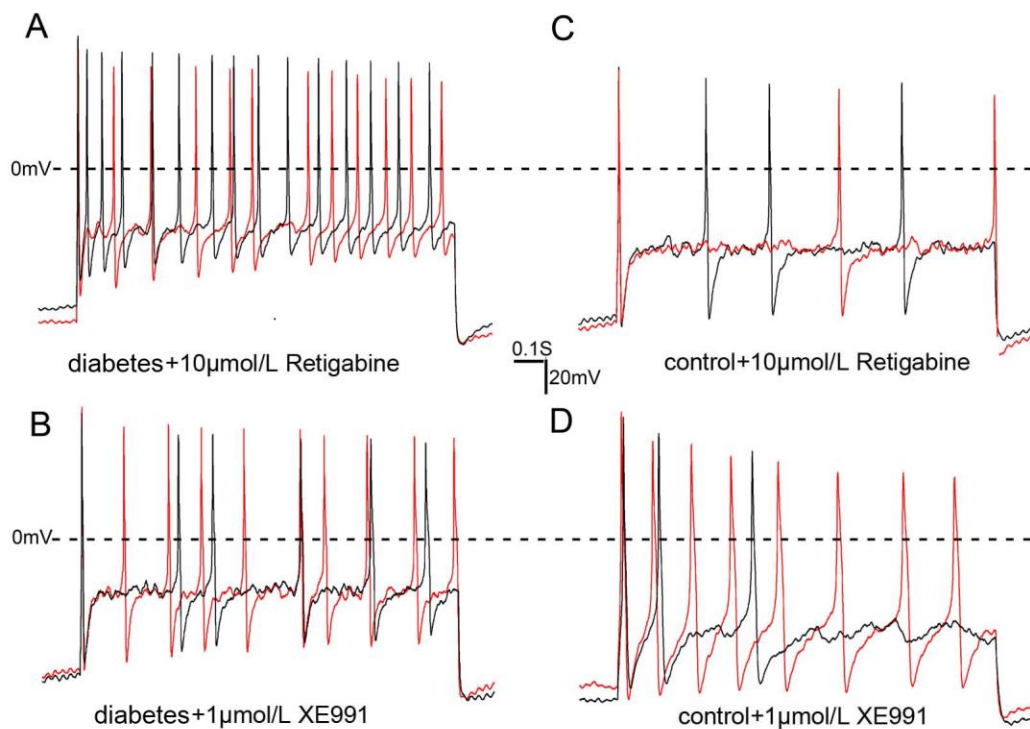


Fig. 6 Excitability of DRG neurons and drug influence. (A) A representative example of evoked AP recorded from a DRG neuron (27.3 pF) of diabetic rat before (black) and after (red) perfusion with retigabine (10 $\mu\text{mol/L}$). (B) A representative example of evoked AP recorded from a DRG neuron (32.6 pF) of diabetic rat before (black) and after (red) perfusion of XE991 (1 $\mu\text{mol/L}$). (C) A representative example of evoked AP recorded from a DRG neuron (21.6 pF) of normal control rat before (black) and after (red) perfusion with retigabine (10 $\mu\text{mol/L}$). (D) A representative example of evoked AP recorded from a DRG neuron (34.0 pF) of normal control rat before (black) and after (red) perfusion with XE991 (1 $\mu\text{mol/L}$). (E-G) The quantitative analysis of neuronal excitability, including resting membrane potential, AP threshold, and frequency of AP before and after perfusion with retigabine (10 $\mu\text{mol/L}$) or XE991 (1 $\mu\text{mol/L}$). Bar graphs with error bars represent mean \pm SEM, $n=40$, $*P<0.001$, diabetes vs control, unpaired Student's t -test, others paired Student's t -test.



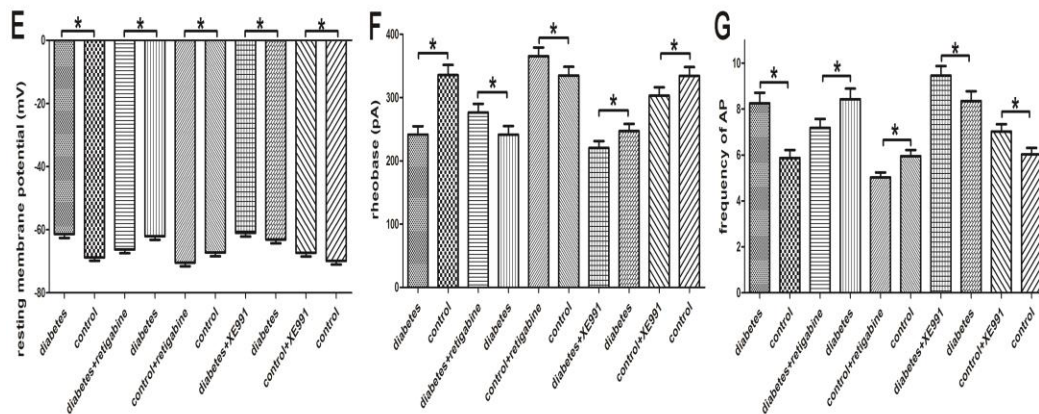


Fig. 7. Paw withdrawal threshold to mechanical and thermal stimulation and drug influence. (A) Paw withdrawal threshold to mechanical stimulation in all groups. (B) Paw withdrawal threshold to thermal stimulation in all groups. Bar graphs with error bars represent mean \pm SEM, $n=20$, * $P < 0.05$, ** $P < 0.01$, *** $P < 0.001$, unpaired Student's t -test.

